

# On the response of a Bose-Einstein condensate exposed to two counterpropagating ultra-fast laser beams

Priyam Das,<sup>1,\*</sup> Ayan Khan,<sup>2,†</sup> and Anirban Pathak<sup>3,‡</sup>

<sup>1</sup>*Department of Physics, Amity Institute of Applied Sciences, Amity University, Kolkata-700156, India.*

<sup>2</sup>*Department of Physics, School of Engineering and Applied Sciences,  
Bennett University, Greater Noida, UP-201310, India*

<sup>3</sup>*Jaypee Institute of Information Technology, A-10, Sector-62, Noida, UP-201309, India*

The effect of light-matter interaction is investigated for a situation where counter propagating laser pulses of localized nature are incident on the atomic condensate. In contrast to the earlier investigations on the similar systems, it's assumed that the laser beams are ultra-fast and they have a  $\text{sech}^2$  profile. Specifically, we consider a quasi-homogeneous, later extended to inhomogeneous, Bose-Einstein condensate (BEC), which is exposed to two counter propagating orthogonally polarized ultra-fast laser beams of equal intensity. The electromagnetic field creates an optical potential for the Bose-Einstein condensate, which in turn modifies the optical field. Hence, light and matter are found to contentiously exchange energy and thus to modify themselves dynamically. In the inhomogeneous case, a self-similar method is used here to treat a cigar-shaped BEC exposed to light. Our theoretical analysis in a hitherto unexplored regime of BEC-light interaction hints at the solitonic bound state formation in the regime where the atom-atom interaction is repulsive and the light-matter interaction is attractive. The energy diagram also indicates a transfer of energy from photon to atom as the light-matter interaction turns repulsive from attractive.

## I. INTRODUCTION

Matter-field interaction is in the heart of spectroscopy and quantum mechanics- Rayleigh scattering to Raman effect, Edington's experimental verification of the general theory of relativity to the recent detection of gravitational waves in LIGO, all are manifestations of matter-field interaction. Interest on matter-field interaction is long and it played a fundamental role in the development of quantum mechanics. Specifically, photoelectric effect and Compton effect are two nice examples of matter-field interaction that played a pivotal role in the development of quantum physics. Later, the interest on matter-field interaction received a boost when laser was discovered in 1960s. Invention of laser helped us to develop new fields like nonlinear optics, quantum optics and atom optics, and thus to reveal true power and beauty of matter-field interaction through the appearance of several new phenomena (cf. [1] and references therein). In fact, advent of laser also helped us in the experimental realization of Bose-Einstein condensates (BECs) as the usual optical trap as well as the optical trap used in MOT (magneto-optical trapping) is realized with laser [2]. It also helped us in realizing ultra-cold gases and super solids and thus opened up a domain of recent interest where we study interaction of light with ultra-cold matter (BEC of different shapes, ultra-cold gases, etc.) [3, 4].

This particular facet of the study of matter-field interaction is interesting for various reasons. For example, in a BEC, it's impossible to distinguish the bosons and thus

to identify- which boson (particle) has scattered a photon. Consequently, a collective scattering occurs and a correlation is developed between the bosons, which subsequently enhances the scattering and may lead to superradiance [5–7] and other phenomena [8]. Specifically, this may help us in realizing the phenomena of nonlinear atom optics and thus to achieve nonlinear phenomena using weak laser source as desired for quantum computation and communication. Further, as the coherence time of BEC is relatively long, they are of particular use in the study of superradiance [9]. However, in a set of recent works [8, 10, 11], the purview of BEC-light interaction has been extended beyond superradiance, and exciting new nonlinear dynamical phenomena have been reported. Particularly, in Ref. [10], a BEC was illuminated by two far off-resonant counter propagating noninteracting laser beams having orthogonal polarization [32], and it was theoretically observed that the spontaneous crystallization of light and ultra-cold atoms may happen. Specifically, in free space, periodic pattern formation for a BEC was reported in a novel regime which was not explored in the earlier works on the self-ordering effect [12–14]. This work established that the possibilities of observing exciting new phenomena in the synthetic solid-state systems may be investigated through the quantum simulations with ultra-cold atoms in optical lattices [10]. Subsequently, the same system was numerically investigated in Ref. [11] to reveal the growth dynamics involved in the self-ordering (spontaneous crystallization) process mentioned above. Specifically, the investigation was focused on a set of experimentally realizable witnesses which can be used to monitor the growth and properties of the crystal formed in the process mentioned above. A similar system was also studied experimentally in [8] by Dimitrova et al. In fact, they considered a physical system composed of an elongated BEC exposed to two counter

\*pdas2@kol.amity.edu

†ayan.khan@bennett.edu.in

‡anirban.pathak@gmail.com

propagating laser beams (along the long axis of the BEC) which were detuned by 160 MHz from each other and by 1-20 GHz from the atomic resonance at 671 nm [8]. Further, an analogous system was studied in Ref. [15] in the context of a one-dimensional Coulomb crystal. The exchanges of energy and momentum through coherent scattering of light from ultra-cold atoms are usually found to introduce different types of nonlinear dynamical effects. The richness of the subject has further been exposed through the investigation of optomechanical strain observed in the ultra-cold atomic cloud [16]. Moreover, in the recent years, ultra-cold atomic gases have also been used as emulators for different condensed matter systems. The idea of emulation is also extended to understand the behavior of electrons in solids when subjected to a strong electric field by means of applying ultra-fast laser field on atomic condensate [17, 18]. The potential of matter-field interaction has broadened further with the proposition of creating and analyzing the anti-matter condensate such as Positronium condensate (PsC) [19]. Since PsC has a very high critical temperature (14K), but very short (142ns) life-time, it's a big challenge to cool the PsC at cryogenic temperature with high density ( $10^{18}/cc$ ). In this regard, the interaction of the anti-matter with the ultra-fast laser pulses is expected to help in realizing PsC and other anti-matter condensates. Motivated by these recent studies [8, 10, 11, 15], in what follows, we study the possibility of production of localized structures in BEC under the influence of two ultra-fast counter propagating non-interating laser beams (say,  $Ti : Al_2O_3$  laser).

As mentioned above, in this article, we aim to investigate the possibility of observing localized structures in BEC under the influence of ultra-fast counter propagating non-interating laser beams. The system is analogous to the physical system discussed in [8, 10, 11]. However, the approach adopted and the region explored is different and consequently, it is expected to reveal new insights. To be precise, till date, ultra-fast laser pulses are rarely used to study the condensate dynamics. However, a better understanding of ultra-fast laser-condensate interaction may yield new insights into the field of ultra-cold hybrid atom-ion system. Here, we investigate the effect of light-matter interaction when ultra-fast laser pulses of localized nature are incident on the atomic condensate. In what follows, we will show that our theoretical analysis hints at the solitonic bound state formation for attractive light-matter interaction. The energy diagram also indicates a transfer of energy from photon to atom as the light-matter interaction turns repulsive from attractive.

The rest of the paper is organized as follows. In Section II, we explicate the model where we briefly describe the dimensional reduction method to reduce the condensate from 3+1 to 1+1 dimension. Also we describe the nature of the potentials present in the system. In Section III, we report the localized solution for the condensate as a result of light-matter interaction. We further probe the localized structure by examining its dispersion and matter-field energy exchange in Section IV. In the penul-

timate section, we extend our investigation to the study of inhomogeneous condensate (Section V). Finally, the paper is concluded in Section VI.

## II. THE MODEL

As stated above, for the present study, we consider a trapped atomic BEC interacting with two counter propagating orthogonally polarized ultra-fast laser beams. The EM field generates an optical potential for the BEC, which in turn modifies the optical field. Consequently, the model system would allow light and matter to contentiously exchange energy and thus to dynamically modify each other.

The BEC can be treated within the purview of the mean-field formalism provided by Gross and Pitaevskii (GP) [20, 21] such that,

$$i\hbar \frac{\partial \Psi(\mathbf{r}, t)}{\partial t} = \left[ -\frac{\hbar^2}{2m} \nabla^2 + U|\Psi(\mathbf{r}, t)|^2 + V(\mathbf{r}) - \nu \right] \Psi(\mathbf{r}, t), \quad (1)$$

where  $U = 4\pi\hbar^2 a_s/m$ ,  $a_s$  being the s-wave scattering length,  $\nu$  is the chemical potential and  $m$  being the mass of the each atom. Further,  $V(r) = V_T(y, z) + V_L(x)$  defines the external potentials, which include the external transverse confinement ( $V_T(y, z) = \frac{1}{2}m\omega_\perp^2(y^2 + z^2)$ ) with  $\omega_\perp$  being the transverse trap frequency, as well as the longitudinal confinement ( $V_L(x)$ ). The potential along the longitudinal direction,  $V_L(x) = V_{HO}(x) + V_{opt}(x)$ , comprises of the harmonic trap  $V_{HO}(x) = \frac{1}{2}m\omega_0^2 x^2$  with  $\omega_0$  being the longitudinal trap frequency, and  $V_{opt}$  being the optical potential created due to the presence of the counter-propagating ultra-fast lasers. It is worth highlighting that the transverse trapping frequency ( $\omega_\perp \sim 2\pi \times 140$  Hz) is much stronger compared to the longitudinal frequency ( $\omega_0 \sim 2\pi \times 8$  Hz). This implies that the interaction energy of the atoms is much less than the kinetic energy in the transverse direction. Consequently, it is possible to reduce Eq.(1) from 3 + 1 dimension to 1 + 1 dimension. In order to reduce Eq.(1) to the corresponding quasi one-dimensional case, we have made use of the following ansatz,

$$\Psi(\mathbf{r}, t) = \frac{1}{\sqrt{2\pi a_B a_\perp}} \psi\left(\frac{x}{a_\perp}, \omega_\perp t\right) e^{\left(-i\omega_\perp t - \frac{y^2 + z^2}{2a_\perp^2}\right)}, \quad (2)$$

where  $a_B = 5.3 \times 10^{-9}$  cm is Bohr radius and  $a_\perp = \sqrt{\frac{\hbar}{m\omega_\perp}}$ .

Applying the ansatz (2) in Eq.(1) we obtain the quasi one dimensional (cigar-shaped) GP equation, describing the dynamics of BEC as follows

$$i\frac{\partial \psi(x, t)}{\partial t} = \left[ -\frac{1}{2} \frac{\partial^2 \psi(x, t)}{\partial x^2} + \frac{1}{2} M x^2 + \tilde{V}_{opt} \right] \psi(x, t) + g|\psi(x, t)|^2 \psi(x, t) - \tilde{\nu} \psi(x, t), \quad (3)$$

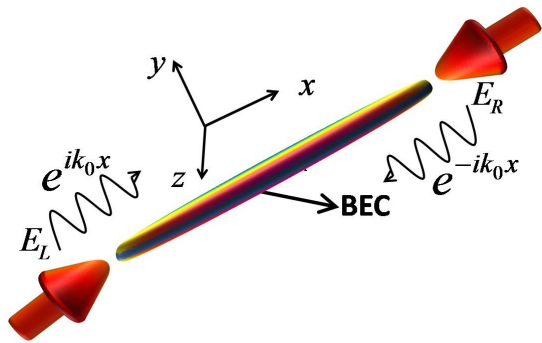


FIG. 1: (Color online) Schematic diagram of the physical system considered here. A cigar-shaped BEC is exposed to two counter-propagating laser beams. In this work, we have considered  $|E_L(x)| = |E_R(x)|$ .

where  $g = 2a_s/a_B$ ,  $M = \omega_0^2/\omega_\perp^2$ ,  $\tilde{V}_{\text{opt}} = V_{\text{opt}}/(\hbar\omega_\perp)$   $\tilde{\nu} = \nu/(\hbar\omega_\perp)$ . Here it is important to note that  $x$  and  $t$  are now actually dimensionless, i.e.  $x \equiv x/a_\perp$  and  $t \equiv \omega_\perp t$ . From here onward, we will follow this dimensionless notation of  $x$  and  $t$ . To begin with, we would concentrate on the dynamics of the condensate in the absence of the harmonic confinement (i.e., when  $M = 0$ ) and would assume that the BEC experiences only the optical potential. However, in the later part of our analysis, we will remove this assumption and explore the trapped scenario ( $M \neq 0$ ) as well, keeping in mind the fact that most of the atomic systems are inhomogeneous.

The quasi one-dimensional BEC described above is considered to be exposed to two counter-propagating ultra-fast laser pulses of equal intensity, as illustrated in Fig.(1) and described in the previous section. The lasers are far detuned from the atomic resonance such that the possibilities of atomic excitation and spontaneous emission from the atoms can be ignored. The impinging laser fields from the left ( $E_L(x, t)$ ) and right ( $E_R(x, t)$ ) can be assumed to be of the form  $E_L(x, t) = [E_{L,R}(x)e^{i\omega_1 t} + \text{c.c.}]$  and  $E_R(x, t) = E_L(x, t)e^{i\pi/2}$ , with  $\omega_1$  being the frequency of the laser pulses. The envelop of the two fields would follow the following Helmholtz equation

$$\frac{\partial^2 E_{L,R}(x, t)}{\partial x^2} - \epsilon(x)\mu \frac{\partial^2 E_{L,R}(x, t)}{\partial t^2} = 0,$$

which can be expressed for the current system as [10],

$$\frac{d^2 E_{L,R}(x)}{dx^2} + k_0^2(1 + \chi(x))E_{L,R}(x) = 0. \quad (4)$$

Here,  $\chi(x)$  is arising as a result of nonlinear effect induced by the propagation of an intense laser beam through BEC medium and it is defined as,  $\chi(x) = \alpha \frac{|\psi(x)|^2}{|\psi_0|^2}$ .  $k_0$  is the wave number of the incoming beams,  $\alpha$  is the strength of atom-light coupling and  $|\psi_0|^2$  is the background density of the condensate. So for a known spatial distribution of

the incoming beam we can determine the optical potential experienced by the BEC as

$$\begin{aligned} V_{\text{opt}}(x) &= \frac{\alpha}{\hbar\omega_\perp} (|E_L(x)|^2 + |E_R(x)|^2) \\ &= \tilde{\alpha}|E(x)|^2, \end{aligned} \quad (5)$$

where we assume that the intensity of the left and right laser pulses are the same,  $|E_L(x)|^2 = |E_R(x)|^2 \equiv |E(x)|^2$  and  $\tilde{\alpha} = 2\alpha/(\hbar\omega_\perp)$ . For notational convenience, we now drop the ‘tilde’, wherever applicable. In the following section we would provide the method to obtain analytical solution of the model system described here.

### III. SOLUTIONS

In the recent studies, where periodic pattern formation has been observed due to light-matter interaction, the impinging laser fields from the left and right were approximated by plane waves, albeit the most common intensity profile happens to be Gaussian. However, the situation is different for pico/femto-second lasers. The intensity profile of the ultra-short pulses can often be better approximated by a  $\text{sech}^2$  function [22]. Therefore, in the present study, we assume the pulse profile to be

$$\begin{aligned} I(x) &= |E(x)|^2 \\ &= \sigma_0 \cos^2 \theta \cosh^{-2} \left( \frac{\cos \theta}{\zeta} (x - ut) \right). \end{aligned} \quad (6)$$

The profile is presented here in the co-moving frame as in what follows, we have conducted our analysis in that frame. Here,  $\sigma_0$  is the constant amplitude related to the background density of the condensate,  $\theta$  is the Mach angle, and  $\zeta$  is the coherence length. In what follows, we would show graphically that the laser profile actually create an optical potential of bell type or Pösch-Teller type.

The condensate wave function can now be considered as combination of a slow moving density part and a fast moving phase part such as  $\psi(x, t) = \rho_a(x, t)e^{i\chi_a(x, t)}$ . Applying this ansatz in Eq.(3) and separating the equation in real and imaginary parts, we obtain phase equation as,  $v = \frac{\partial \chi_a}{\partial \eta} = u(1 - \frac{\rho_0^2}{\rho_a^2})$ , where  $\eta = x - ut$ . In terms of density, we can rewrite the equation as,  $v = u(1 - \frac{\sigma_0}{\sigma_a})$ , where  $\rho_0 = \sqrt{\sigma_0}$  and  $\rho_a = \sqrt{\sigma_a}$ .

The real part of the GP equation yields,

$$\begin{aligned} -\frac{1}{4}\sigma_a \frac{d^2 \sigma_a}{d\eta^2} + \frac{1}{8} \left( \frac{d\sigma_a}{d\eta} \right)^2 + g\sigma_a^3 + \alpha\sigma_b\sigma_a^2 \\ - \left( \frac{u^2}{2} + \nu \right) \sigma_a^2 + \frac{u^2}{2} \sigma_0^2 = 0. \end{aligned} \quad (7)$$

We now consider an ansatz of localized solution with background density  $\sigma_0$  as

$$\sigma_a = \sigma_0 \left( 1 - \cos^2 \theta \cosh^{-2} \left( \frac{\cos \theta}{\zeta} \eta \right) \right). \quad (8)$$

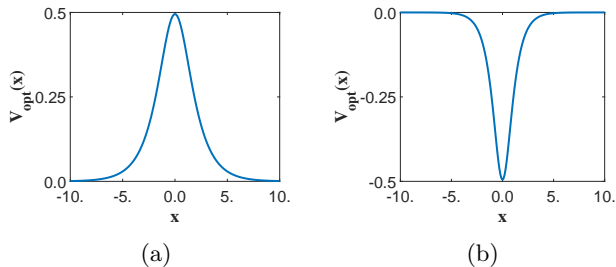


FIG. 2: (a) The effective bell type optical potential generated due to the light-matter interaction. Here, both  $g$  and  $\alpha$  are repulsive (positive), but  $\alpha < g$ . We have used an arbitrary value for light-matter coupling strength i.e.  $\alpha = 0.5$ . (b) The effective Pösch-Teller type optical potential is generated due to the light matter interaction. Here  $g$  ( $\alpha$ ) corresponds to a repulsive (attractive) interaction. Here we consider  $\alpha = -0.5$ . In both figures  $g = 1$ .

Applying this ansatz in Eq.(7) we obtain a set of consistency conditions like, the background density is controlled by the atom-atom short range interaction and the chemical potential ( $\sigma_0 = \nu/g$ ), the coherence length can be defined as  $\zeta = \frac{1}{\sqrt{(g-\alpha)\sigma_0}}$  and the wave number  $k_0^2 = \frac{1}{2}\kappa\sigma_0(\cos^2\theta - 2)$ , where  $\kappa = 2(-g + \alpha)$ . The Mach angle would be defined as the ratio of soliton velocity and the sound velocity such that  $\sin\theta = \frac{u}{u_s}$ , where the sound velocity  $u_s = \sqrt{(g-\alpha)\sigma_0}$ . As the coherence length is always positive, we obtain several possible interaction regimes corresponding to the allowed relations between atom-atom coupling strength  $g$  and light-matter coupling strength  $\alpha$ , which are required to satisfy  $|g - \alpha| > 0$ . Let us now elaborate each of these possibilities:

- Case I:  $g > 0$ ,  $\alpha > 0$ , but  $\alpha < g$ ; this implies that atom-atom interaction as well as light-matter interaction is repulsive. In this case, the effective optical potential behaves like a barrier as illustrated in Fig. 2(a).
- Case II: Contrary to the previous case, for  $g > 0$  and  $\alpha < 0$  the effective optical potential turns out to be Pösch-Teller type which can support a bound state formation (see Fig. 2 (b)). In both the cases for  $\alpha \rightarrow 0$  the coherence length and the sound velocity takes the usual form for homogeneous BEC.
- Case III: It is also possible that for an attractive BEC, the light-matter interaction is also attractive. However, in that case, for a physically meaningful result, we should have  $|\alpha| > |g|$ . The effective optical potential is again Pösch-Teller type. Here it is worth mentioning that  $\alpha \rightarrow 0$  would lead to unphysical consequences with complex coherence length and sound velocity. However,  $g \rightarrow 0$  may

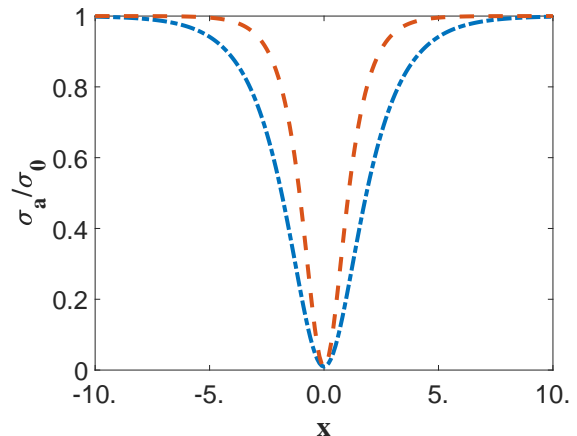


FIG. 3: (Color online) Variation of the dark soliton width due to attractive and repulsive photon-atom coupling. The dashed and dashed-dotted line correspond to  $\alpha = -0.5g$  and  $\alpha = 0.5g$  respectively. We used an arbitrary repulsive value for  $g$  and  $g = 1$ .

be physically relevant in a situation where the non-interacting ultra-cold atomic gases are considered to be trapped in an optical potential.

- Case IV: One can also think of a situation when the atom-atom interaction is attractive, but the light-matter interaction is repulsive. In that case, the coherence length and sound velocity become complex quantities, thereby leads to an unphysical domain. Hence, we ignore this case.

To visualize the different regimes of the light-matter interaction involved in the physical system of our interest, Eq.8 is plotted in Fig. 3 for two different regimes. It is clear from the figure that the total number of particle ( $N = \int |\psi|^2 dx$ ) is less in the attractive regime. However, the figure does not carry the necessary information regarding the loss of atom. Therefore, it is important to analyze the energy and momentum of the solitonic excitations in BEC. In the following section, we have done the same.

#### IV. ENERGY OF THE SOLITONIC MODE

To analyze the solitonic mode, which is gray in nature under the influence of ultra-short laser pulses, we minimize the energy and compute the energy functional as,

$$E_a = \frac{1}{2} \int \left( \frac{\partial \psi^*}{\partial x} \right) \left( \frac{\partial \psi}{\partial x} \right) dx + \frac{g}{2} \int (\psi^* \psi)^2 dx + \alpha \int (E_L^* E_L) (\psi^* \psi) dx - \nu \int (\psi^* \psi) dx. \quad (9)$$

Subsequently, using Eqs. (8) and (9) and subtracting the background we obtain

$$E_a = \frac{4}{3}g\sigma_0^2\zeta \cos^3\theta + 2\alpha\sigma_0^2\zeta \left( \cos\theta - \frac{2}{3}\cos^3\theta \right). \quad (10)$$

Corresponding momentum can be written as

$$P_a = -i \int \psi^* \frac{\partial\psi}{dx} dx \\ \sigma_0 \left( \pi \frac{u}{|u|} - 2\theta - \sin 2\theta \right). \quad (11)$$

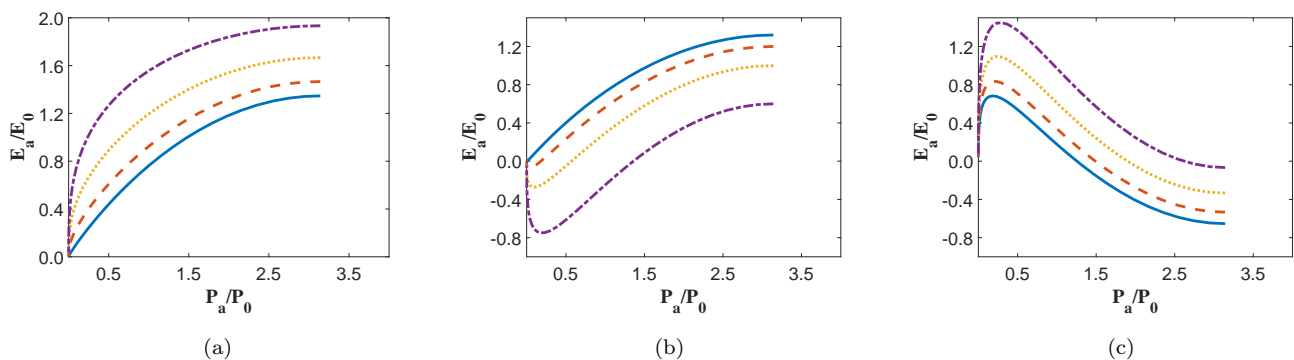


FIG. 4: (Color online) The energy momentum dispersion of the matter wave when the repulsive BEC is subjected to an effective optical potential of bell type (Case I), Pösch-Teller type (Case II) and attractive BEC experiences an optical potential of Pösch-Teller type (Case III). Here  $E_0 = \sigma_0^2\zeta$  and  $P_0 = \sigma_0\hbar$ . In (a) solid line corresponds to  $\alpha = 0.02g$ , dashed line is for  $\alpha = 0.2g$ , the dotted line depicts  $\alpha = 0.5g$  and dispersion with  $\alpha = 0.9g$  is presented using dashed dotted line. Similarly, in (b) solid line corresponds to  $\alpha = 0.02g$ , dashed line is for  $\alpha = 0.2g$ , the dotted line depicts  $\alpha = 0.5g$  and dispersion with  $\alpha = 1.1g$  is presented using dashed dotted line. In (c)  $|\alpha| > |g|$  and thus the solid line, dashed line, dotted line and dashed dotted line represent  $\alpha = -1.02g$ ,  $\alpha = -1.2g$ ,  $\alpha = -1.5g$  and  $\alpha = -1.9g$ , respectively.

The energy vs momentum dispersion curves for the above mentioned cases are depicted in Fig. 4. In Fig. 4(a), the dispersion curve is given for Case I and we observe the well known  $2\pi$  periodicity, thereby affirming the prediction of Lieb [23, 24]. Nevertheless, the maximum energy corresponding to  $\pi$  momentum differs considerably based on the strength of  $\alpha$ . The situation is quite different for repulsive BEC with attractive light matter interaction (see Fig. 4(b)). The competition between  $g$  and  $\alpha$  leaves signature of solitonic bound state formation at low momentum with sufficiently high  $\alpha$  (when  $|\alpha|$  is of the order of  $\sim 0.2g$  or above). This is also consistent with the fact that the atom number is less for attractive  $\alpha$  as described in Fig. 3. However, at high momenta the system tries to follow its usual path. For attractive BEC with an attractive light-matter interaction, the situation is reversed which can be observed from Fig. 4(c). The dispersion is highly nonlinear at low momenta. How-

ever, for high momenta, it tends to form bound states by virtue of strong attractive interaction between the atoms. However, strong light-matter attractive interaction tries to oppose this.

It is worth noticing that in Case II, we do not have any constraints on the strength of  $g$  and  $\alpha$ . Further, the dispersion diagram for this regime indicates bound state formation for solitons. Hence, this regime demands more attention. To reveal the interplay between the two interactions, where one ( $g$ ) tries to delocalize the solitons and the other ( $\alpha$ ) tries to localize them, it is important that we study the energy transfer mechanism between light and matter. For this purpose, we calculate the photon

energy ( $E_P$ ) which is defined as,

$$\begin{aligned} E_P &= \frac{k_0^2}{2} \int (1 + \chi(x)) E_L^* E_L dx \\ &= k_0^2 \sigma_0 \zeta \cos \theta + \frac{2}{3} \alpha k_0^2 \sigma_0 \zeta \cos \theta (2 \cos^2 \theta - 3), \end{aligned} \quad (12)$$

and plot  $E_a$  and  $E_P$  with varying  $\alpha$  (see Fig. 5) for three different values of atom-atom interaction strength. In general, we observe that photon energy decreases as an effect of tuning  $\alpha$  from attractive to repulsive, whereas soliton energy is found to increase for the same situation. This clearly suggests the occurrence of energy transfer from photon to soliton.

In Fig. 5 the energy is normalized by  $\sigma_0^2 \beta$  where  $\zeta = \beta / \sqrt{(g - \alpha)}$  and  $\beta = 1 / \sqrt{\sigma_0}$ . In the left most figure (Fig. 5(a)), we again observe the signature of solitonic

bound state formation for attractive  $\alpha$  while  $g$  is moderately weak ( $g = 0.5$ ) (as pointed out in Fig. 4(b) as well). However, as we increase the repulsive strength of  $g$  this signature quite naturally evaporate (see Fig.5(b) and (c)). Interestingly, strong atom-atom and light-matter repulsive interaction encourages the photons to form bound state which can be observed in Fig. 5(c).

However, against our expectation the total energy shows a nonmonotonic behavior. The energy minimum lies in the vicinity of  $\alpha \rightarrow 0+$  which indicates the most stable region of the system. The attractive  $\alpha$  supports the bound state formation of solitons, but they may lead to dynamical instability in the system and resulting in dissipative motion of the BEC [25]. Therefore, the weak repulsive  $\alpha$  allows the system to be more stable. Increasing the light-matter repulsive interaction further, one can destabilize the system again.

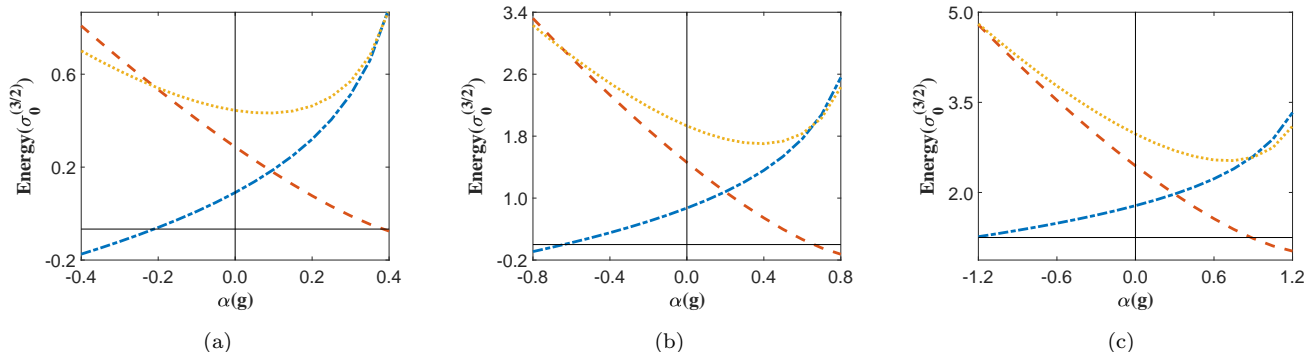


FIG. 5: (Color online) This figure depicts energy variation of solitonic mode and photonic mode as light-matter interaction is tuned ( $\alpha$ ). In all the figures the dashed-dotted line represents soliton energy, dashed line is for photon energy and the sum of these two energies is illustrated through dotted line. Across the figures  $\alpha$  is varied as a function of  $g$ , to be precise from  $-0.8g$  to  $0.8g$ . The value of  $g$  from left to right is as follows: 0.5, 1.0, 1.5. All the energies are in units of  $\sigma_0^2 \beta$ .

## V. INHOMOGENEOUS BEC

The analysis performed until this point has been carried out by considering only an effective optical potential. A more practical situation would be one in which the atoms are trapped in a parabolic potential. In this section, we describe a method that allows us to study such a physical situation. In such a scenario, the quasi one-dimensional nonlinear Schrödinger equation with a harmonic trap would take the following form

$$i \frac{\partial \psi(x, t)}{\partial t} = \left[ -\frac{1}{2} \frac{\partial^2 \psi(x, t)}{\partial x^2} + \frac{1}{2} M(t) x^2 + V_{\text{opt}} \right] \psi(x, t) + \tilde{g}(t) |\psi(x, t)|^2 \psi(x, t) - \nu(t) \psi(x, t) \quad (13)$$

In order to solve this nonlinear equation, we may adopt a self-similar method, where the effect of the trap is embedded in the chirping of the wave function. This method further allows us to consider a more generic type of interaction and trap geometry which can change with time as noted in Eq.(13). In what follows, we will further elaborate the effectiveness of these assumptions. In fact, this method has already been elaborated in a number of papers [26–29]. In the present case, the optical potential need to be time-dependent,  $V_{\text{opt}}(x, t) = 2\tilde{\alpha}(t)|E(x)|^2$ , where  $\tilde{\alpha}(t)$  mimics the time-dependent interaction between the condensate atoms and the optical field. In this approach, we can assume the following solution

$$\psi(x, t) = \sqrt{A(t)\sigma(\xi)} e^{i[\chi(\xi) + \Phi(x, t)]}, \quad (14)$$

where we describe the dynamics of the solitons in center of mass (CoM) frame such that,  $\xi(x, t) = A(t)(x - l(t))$ . Here,  $A(t)$  can be considered as the inverse of width and  $l(t)$  as the position of the condensate in the CoM frame. The kinematic phase  $\Phi(x, t)$  has a quadratic form:  $\Phi(x, t) = -\frac{1}{2}c(t)x^2$ , exhibiting chirping.

From current conservation, amounting to solve the imaginary part of the GP equation, one obtains,  $\frac{\partial \chi(\xi)}{\partial \xi} = u(1 - \frac{\sigma_0}{\sigma(\xi)})$ , where  $\sigma_0$  is the Thomas-Fermi background density of the condensate atoms in the CoM frame  $\xi(x, t)$ . The coefficient of chirping  $c(t)$  can be determined from the following Riccati-type equation,  $\frac{\partial c(t)}{\partial t} - c^2(t) = M(t)$ , which is obtained by using the self-similar method. It is worth pointing out that the above Riccati-type equation can be expressed as a Schrödinger eigenvalue problem by incorporating the appropriate transformation as shown in [26]. In this frame, the density equation (real part of the nonlinear Schrödinger equation) can be cast in the convenient form [24],

$$\begin{aligned} & -\frac{1}{4}\sigma_a \frac{d^2\sigma_a}{d\eta^2} + \frac{1}{8}\left(\frac{d\sigma_a}{d\eta}\right)^2 + \kappa\sigma_a^3 + \alpha\sigma_b\sigma_a^2 \\ & - \left(\frac{u^2}{2} + \mu\right)\sigma_a^2 + \frac{u^2}{2}\sigma_0^2 = 0. \end{aligned} \quad (15)$$

where  $g(t) = g_0 e^{-G} A(t)/A_0$  with  $\kappa = g_0/A_0$ . Here  $\mu = \nu(t)/A^2(t)$  and  $\alpha = \alpha(t)/A^2(t)$  are the chemical potential and the scaled light-matter interaction in the moving coordinate frame.

The inverse of width follows the equation:  $\partial A(t)/\partial t = A(t)c(t)$ , which can be used to obtain  $A(t)$ , once the chirping  $c(t)$  is determined from the Riccati equation. For better understanding, we separate the governing equation of the CoM motion:  $\frac{\partial l(t)}{\partial t} + c(t)l(t) = A(t)u$ . Kohn theorem [30] states that the CoM motion oscillates exactly with the trap frequency. The same is observed in Fig. 6. When the trap frequency varies with time, the CoM motion ceases to decouple from the trap, leading to a nontrivial behavior as discussed in detail by some of the present authors in [31]. Further, we would like to note that similar oscillatory behavior was observed even in the case of unitary Fermi gas in the realm of extended Thomas Fermi density functional theory [29]. The time modulated trapping frequency is coupled with the spatio-temporal dynamics of the condensates and soliton-like excitations in the following way,

$$\frac{\partial^2 l(t)}{\partial t^2} + M(t)l(t) = 0. \quad (16)$$

Now we must take a note of Eq.(15) which is exactly the same as Eq.(7). Hence, it is quite natural that the discussions in the previous two sections can be extended for the trapped system. For sake of completeness we note that the soliton solution obtained from Eq. (15) takes self-similar form,

$$\sigma(\xi) = \sigma_0 - \sigma_0 \cos^2 \theta \operatorname{sech}^2 \left[ \frac{\cos \theta}{\zeta} \xi(x, t) \right], \quad (17)$$

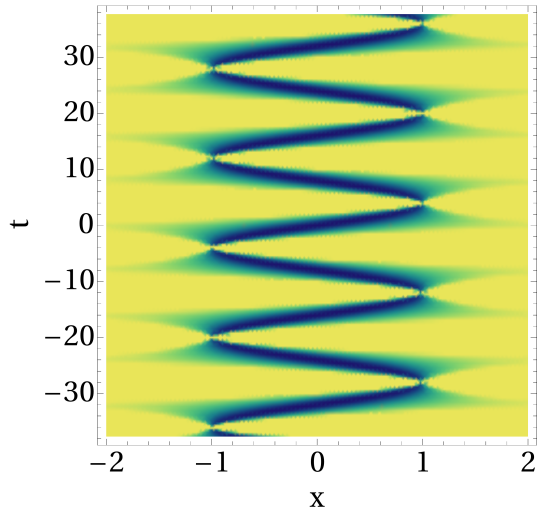


FIG. 6: (Color online) Oscillation of a dark soliton in a harmonic trap. The figure is prepared for a situation discussed in Case II. Specifically, for  $\alpha = -0.5g$  and considering an arbitrary value for  $g$  as  $g = 1$ ; coherence length is scaled by  $\beta = 1/\sqrt{\sigma_0}$ . The  $x$  and  $t$  are dimensionless as mentioned in Section II.

where the Mach angle is given by,  $\theta = \sin^{-1} \frac{V}{U_s} = \sin^{-1} \frac{u}{u_s}$ . Here,  $V = A(t)u$  is the velocity of the solitons in the presence of the harmonic trap, which is bounded by a maximum velocity  $U_s = A(t)u_s$ , with  $u_s$  being the maximum velocity of the soliton in the absence of the harmonic trap.

In this section, we have explicated an analytical method to deal with the external trapping potential and showed that our method actually maps it to the homogeneous system without losing the essence of the trap. Only constrain remain is that, the system must abide by the consistency conditions mentioned above. Nevertheless it is now obvious that the response of the condensate to ultra-fast laser will follow the same suit as described in Section IV.

## VI. CONCLUSION

In the present work, we have investigated the effect of counter propagating ultra-fast laser beams on atomic condensate. The intensity profile of the lasers has a localized structure and shining them on the condensate results in generation of dark/gray solitons. We start from the three dimensional GP equation and briefly describe the method of dimensional reduction for a cigar-shaped BEC. Later, we consider that the longitudinal trapping potential is substantially weak, such that we can consider the system as quasi-homogeneous. We then show that the localized profile of the laser beam actually induces localized structures in the condensate, which we identify as dark/gray soliton. We have also observed that there ex-

ists a competition between atom-atom coupling strength,  $g$  and light-matter coupling strength  $\alpha$ . Hence, we study the energy exchange process between the laser light and the atomic condensate. Interestingly, against our expectation we have observed a nonmonotonic nature in total energy. This suggests that the system is most stable for repulsive BEC with repulsive (small) light-matter interaction. In general, the light energy is gradually transferred to the atomic condensate as we move from negative  $\alpha$  to positive  $\alpha$ . Since the attractive  $\alpha$  connects with a Pösch-Teller type optical potential, it supports solitonic bound state formation. This signature of that is witnessed through Fig. 4(b) and 5(a).

In short, we would like to emphasize that our analysis has revealed that the ultra-fast light-BEC interaction

can be investigated in multiple regimes and meticulous understanding of physical phenomena happening at each of these regimes requires urgent attention. We believe that our current study would provide some insight into this issue and initiate an intense effort to examine novel aspects of light-matter physics.

### Acknowledgement

Authors acknowledge insightful discussions with P. K. Panigrahi. AP also thanks Department of Science and Technology (DST), India for the support provided through the project number EMR/2015/000393.

- 
- [1] Anirban Pathak and Ajoy Ghatak. Classical light vs. nonclassical light: characterizations and interesting applications. *Journal of Electromagnetic Waves and Applications*, 32(2):229–264, 2018.
- [2] Axel Griesmaier, Jörg Werner, Sven Hensler, Jürgen Stuhler, and Tilman Pfau. Bose-einstein condensation of chromium. *Physical Review Letters*, 94(16):160401, 2005.
- [3] Igor B Mekhov and Helmut Ritsch. Quantum optics with ultracold quantum gases: towards the full quantum regime of the light-matter interaction. *Journal of Physics B: Atomic, Molecular and Optical Physics*, 45(10):102001, 2012.
- [4] Crispin Gardiner and Peter Zoller. The quantum world of ultra-cold atoms and light book ii: The physics of quantum-optical devices. In *The Quantum World of Ultra-Cold Atoms and Light Book II: The Physics of Quantum-Optical Devices*, pages 1–524. World Scientific, 2015.
- [5] H Keßler, J Klinder, M Wolke, and A Hemmerich. Steering matter wave superradiance with an ultranarrow-band optical cavity. *Physical Review Letters*, 113(7):070404, 2014.
- [6] Patrizia Weiss, Michelle O Araújo, Robin Kaiser, and William Guerin. Subradiance and radiation trapping in cold atoms. *New Journal of Physics*, 20(6):063024, 2018.
- [7] Liangchao Chen, Pengjun Wang, Zengming Meng, Lianghai Huang, Han Cai, Da-Wei Wang, Shi-Yao Zhu, and Jing Zhang. Experimental observation of one-dimensional superradiance lattices in ultracold atoms. *Physical Review Letters*, 120(19):193601, 2018.
- [8] Ivana Dimitrova, William Lunden, Jesse Amato-Grill, Niklas Jepsen, Yichao Yu, Michael Messer, Thomas Rigaldo, Graciana Puentes, David Weld, and Wolfgang Ketterle. Observation of two-beam collective scattering phenomena in a bose-einstein condensate. *Physical Review A*, 96(5):051603, 2017.
- [9] MG Moore and Pierre Meystre. Theory of superradiant scattering of laser light from bose-einstein condensates. *Physical Review Letters*, 83(25):5202, 1999.
- [10] Stefan Ostermann, Francesco Piazza, and Helmut Ritsch. Spontaneous crystallization of light and ultracold atoms. *Physical Review X*, 6(2):021026, 2016.
- [11] S Ostermann, F Piazza, and H Ritsch. Probing and characterizing the growth of a crystal of ultracold bosons and light. *New Journal of Physics*, 19(12):125002, 2017.
- [12] Peter Domokos and Helmut Ritsch. Collective cooling and self-organization of atoms in a cavity. *Physical Review Letters*, 89(25):253003, 2002.
- [13] Adam T Black, Hilton W Chan, and Vladan Vuletić. Observation of collective friction forces due to spatial self-organization of atoms: from rayleigh to bragg scattering. *Physical Review Letters*, 91(20):203001, 2003.
- [14] KJ Arnold, MP Baden, and MD Barrett. Self-organization threshold scaling for thermal atoms coupled to a cavity. *Physical Review Letters*, 109(15):153002, 2012.
- [15] Julian Schmidt, Alexander Lambrecht, Pascal Weckesser, Markus Debatin, Leon Karpa, and Tobias Schaetz. Optical trapping of ion coulomb crystals. *Physical Review X*, 8(2):021028, 2018.
- [16] Noam Matzliah, Hagai Edri, Asif Sinay, Roei Ozeri, and Nir Davidson. Observation of optomechanical strain in a cold atomic cloud. *Physical Review Letters*, 119(16):163201, 2017.
- [17] Shankari V Rajagopal, Kurt M Fujiwara, Ruwan Senaratne, Kevin Singh, Zachary A Geiger, and David M Weld. Quantum emulation of extreme non-equilibrium phenomena with trapped atoms. *Annalen der Physik*, 529(8):1700008, 2017.
- [18] Ruwan Senaratne, Shankari V Rajagopal, Toshihiko Shimasaki, Peter E Dotti, Kurt M Fujiwara, Kevin Singh, Zachary A Geiger, and David M Weld. Quantum simulation of ultrafast dynamics using trapped ultracold atoms. *Nature Communications*, 9(1):2065, 2018.
- [19] Kenji Shu, Xing Fan, Takayuki Yamazaki, Toshio Namba, Shoji Asai, Kosuke Yoshioka, and Makoto Kuwata-Gonokami. Study on cooling of positronium for bose-einstein condensation. *Journal of Physics B: Atomic, Molecular and Optical Physics*, 49(10):104001, 2016.
- [20] Eugene P Gross. Structure of a quantized vortex in boson systems. *Il Nuovo Cimento (1955-1965)*, 20(3):454–477, 1961.
- [21] LP Pitaevskii. Vortex lines in an imperfect bose gas. *Sov. Phys. JETP*, 13(2):451–454, 1961.
- [22] Charles Jean Joachain, Niels J Kylstra, and Robert M

- Potvliege. *Atoms in intense laser fields*. Cambridge University Press, 2012.
- [23] Elliott H. Lieb. Exact analysis of an interacting bose gas. ii. the excitation spectrum. *Physical Review*, 130:1616–1624, May 1963.
- [24] AD Jackson and GM Kavoulakis. Lieb mode in a quasi-one-dimensional bose-einstein condensate of atoms. *Physical Review Letters*, 89(7):070403, 2002.
- [25] Biao Wu and Qian Niu. Landau and dynamical instabilities of the superflow of bose-einstein condensates in optical lattices. *Physical Review A*, 64(6):061603, 2001.
- [26] Rajneesh Atre, Prasanta K Panigrahi, and Girish Saran Agarwal. Class of solitary wave solutions of the one-dimensional gross-pitaevskii equation. *Physical Review E*, 73(5):056611, 2006.
- [27] Priyam Das, Ayan Khan, and Prasanta K Panigrahi. Realization of negative mass regime and bound state of solitons in inhomogeneous bose-einstein condensates. *The European Physical Journal D*, 70(5):113, 2016.
- [28] Priyam Das and Prasanta K Panigrahi. Controlled generation of nonlinear resonances through sinusoidal lattice modes in bose-einstein condensate. *Laser Physics*, 25(12):125501, 2015.
- [29] Ayan Khan and Prasanta K Panigrahi. Bell solitons in ultra-cold atomic fermi gas. *Journal of Physics B: Atomic, Molecular and Optical Physics*, 46(11):115302, 2013.
- [30] Walter Kohn. Cyclotron resonance and de haas-van alphen oscillations of an interacting electron gas. *Physical Review*, 123(4):1242, 1961.
- [31] Priyam Das and Prasanta K Panigrahi. Controlled generation of nonlinear resonances through sinusoidal lattice modes in bose-einstein condensate. *Laser Physics*, 25(12):125501, 2015.
- [32] orthogonal polarization was used in [10] and the same is also used in the present work to circumvent the possibility of interference of the counter propagating beams